Probabilistic Push-Over Analysis of Structural and Soil-Structure Systems

M. Barbato, A.M.ASCE[1]; Q. Gu, A.M.ASCE[2]; and J. P. Conte, M.ASCE[3]

Abstract: In this paper, the mean-centered first-order second-moment (FOSM) method is employed to perform probabilistic push-over analysis (POA) of structural and/or soil-structure systems. Approximations of first and second statistical moments (FSSMs) of engineering demand parameters (EDPs) of structural and/or geotechnical systems with random material parameters are computed based on finite-element (FE) response and response sensitivity analysis (RSA) results. The FE RSA is performed accurately and efficiently by using the direct differentiation method (DDM) and is employed to evaluate the relative importance (RI) of the various modeling material parameters in influencing the variability of the EDPs. The proposed approximate methodology is illustrated through probabilistic POA results for nonlinear inelastic FE models of: (1) a three-story reinforced-concrete (RC) frame building and (2) a soil-foundation-structure interaction system consisting of a RC frame structure founded on layered soil. FSSMs of EDPs computed through the FOSM method are compared with the corresponding accurate estimates obtained via Monte Carlo simulation. Results obtained from "exact" (or "local") and "averaged" (or "global") response sensitivities are also compared. The RI of the material parameters describing the systems is studied in both the deterministic and probabilistic sense, and presented in the form of tornado diagrams. Effects of statistical correlation between material parameters are also considered and analyzed by the FOSM method. A simple approximation of the probability density function and cumulative distribution function of EDPs due to a single random parameter at a time (while all the other parameters are fixed to their mean values) is also proposed. Conclusions are drawn on both the appropriateness of using local RSA for simplified probabilistic POA and on the application limits of the FOSM method. It is observed that the FOSM method combined with the DDM provides accurate estimates of FSSMs of EDPs for low-to-moderate level of inelastic structural or system behavior and useful qualitative information on the RI ranking of material parameters on the structural or system response for high level of inelastic behavior.

Introduction

Evaluation of the uncertainty in the computed structural response of civil structures is of paramount importance in order to improve safety and optimize the use of economic resources. In the last two decades, significant research has been devoted to study the propagation of uncertainties from modeling parameters to structural response through the finite-element (FE) method (Dong et al. 1987; Der Kiureghian and Ke 1988; Bjerager 1990; To 2001), leading to FE-based probabilistic methodologies (e.g., the sto-chastic equivalent linearization method, see Ghanem and Spanos 1991, Crandall 2006, and the stochastic perturbation method, see Bolotin 1968, Grigoriu 2000) for computation of the statistics of the random response of structures with uncertain properties and/or subjected to random loading.

This paper presents a comparison of two different probabilistic response analysis (PRA) methods based on quasi-static nonlinear FE response simulation. The mean-centered first-order second-moment (FOSM) approximation (Haukaas and Der Kiureghian 2004) is used to estimate first and second statistical moments (FSSMs) of FE response quantities. These estimates are compared with results obtained using Monte Carlo simulation (MCS) (Liu 2001). The FOSM method requires FE response sensitivity analy-sis (RSA) as a crucial component. In this work, FE response sensitivities are computed using two different methods, namely the direct differentiation method (DDM) (Kleiber et al. 1997) and the finite difference method (FDM). Only material nonlinearities and uncertainties in material parameters are considered in this study, but the employed method can account also for geometric nonlinearities and uncertainties in geometric parameters (Haukaas and Der Kiureghian 2004, 2005).

The FOSM approximation is applied to advanced state-of-the-art nonlinear FE models of realistic structures and soil-structure-foundation interaction (SFSI) systems subjected to quasi-static push-over analysis (POA). Nonlinear POA is a popular procedure in the earthquake engineering community, since it allows gaining

[1]Assistant Professor, Civil and Environmental Engineering, Louisiana State Univ. and A&M College, Baton Rouge, LA 70803. E-mail: mbarbato@lsu.edu

[2]Associate Professor, School of Architecture and Civil Engineering, Xiamen Univ., Xiamen, Fujian, P.R. China 361005; formerly, Postdoc-toral Researcher, Civil and Environmental Engineering, Louisiana State Univ. and A&M College, Baton Rouge, LA 70803 (corresponding author). E-mail: quan.gu.ucsd@gmail.com

[3]Professor, Dept. of Structural Engineering, Univ. of California at San Diego, La Jolla, CA 92093. E-mail: jpconte@ucsd.edu

insight into the nonlinear seismic response behavior of structures using simplified analysis techniques. Even though this procedure presents several shortcomings and provides only a static approximation of the actual dynamic structural behavior, nonlinear POA has been recognized by international codes [Applied Technology Council (ATC) 1996, 2005; BSCC 1997; Chinese Building Press (CBP) 2001; European Committee for Standardization (ECS) 2005] as a possible substitute, under certain conditions, for the more accurate nonlinear dynamic analysis of structural systems.

FE RSA

FE RSA is used in several subfields of structural engineering, such as structural optimization, structural identification, FE model updating, reliability analysis, and is also a crucial ingredient of FOSM analysis. For real-world problems, response simulation (i.e., computation of response quantities $\mathbf{r}=[r_1 r_2 \ldots r_m]^T$ for given values of a set of random parameters $\boldsymbol{\theta}=[\theta_1 \theta_2 \ldots \theta_n]^T$) is typically performed using advanced mechanics-based nonlinear FE models. FE RSA requires augmenting existing (deterministic) FE formulations for response-only calculation with the capability of computing the gradient of the response quantities $\mathbf{r}$ with respect to parameters $\boldsymbol{\theta}$, i.e., $[\nabla_{\boldsymbol{\theta}}\mathbf{r}]_{ij}=\partial r_i / \partial \theta_j$, in which $i=1,2,\ldots,m$ and $j=1,2,\ldots,n$ (in short, the FE response sensitivities to parameters $\boldsymbol{\theta}$).

Several methods are available for computing FE response sensitivities, such as numerical differentiation, the forward/backward/central FDM, and the DDM (Kleiber et al. 1997). The FDM consists of performing one (in the case of forward/backward FDM) or two (in the case of central FDM) FE response analysis by perturbing the value of the sensitivity parameter θ_i $(i=1,\ldots,n)$ by a small but finite amount $\Delta\theta_i$ in addition to a FE analysis with all parameters $\boldsymbol{\theta}$ set at their nominal values. Each response sensitivity is then obtained as the ratio of the response variation and the parameter perturbation. This method is computationally expensive, approximate in nature and potentially suffering from numerical inaccuracies (Haftka and Gurdal 1993; Conte et al. 2003; Zona et al. 2005). On the other hand, the DDM is an accurate and efficient RSA method for nonlinear hysteretic FE models. This method consists of: (1) differentiating analytically the space- and time-discretized equations of motion/equilibrium of the FE model of the considered structural/geotechnical system, and (2) solving the obtained sensitivity equations as the FE analysis proceeds. The response sensitivity computation algorithm requires extending all various hierarchical layers of FE response calculation with the corresponding response derivatives. These layers include the structure, element, integration point (section for frame elements), and material levels. For a detailed explanation of the DDM, the interested reader is referred elsewhere (Kleiber et al. 1997; Conte et al. 1995, 2003, 2004; Haukaas and Der Kiureghian 2004, 2005; Barbato and Conte 2005, 2006; Zona et al. 2005, 2006; Haukaas 2006; Barbato et al. 2007). At the one-time cost of implementing in a FE code the algorithms for analytical differentiation of the FE response, the DDM provides exact response sensitivities (consistent with the numerical response) at a small fraction of the computational cost of the additional FE analyses required by the FDM (Conte et al. 2003; Haukaas and Der Kiureghian 2004; Lupoi et al. 2006). Both the DDM and the FDM with small perturbations compute the "local" (or "exact") response sensitivities of the considered FE model (the DDM in an analytical way, and the FDM in an approximate way). "Global" (or "averaged") response sensitivi-

ties are computed through forward/backward finite difference (FD) analysis using a relatively large parameter perturbation, e.g., equal to one standard deviation (SD) of the random parameter. These averaged sensitivities are insensitive to noise in the computed structural response and approximately account for higher-order terms of the response Taylor series expansion in the perturbation range (e.g., mean ± 1 SD). They can be used as an alternative to local response sensitivities in PRA, but they are not proper global response sensitivities since they do not satisfy the property of multidimensional averaging (simultaneous exploration of all sources of uncertainty) (Saltelli et al. 2000).

Stand-alone FE RSA is also invaluable for gaining deeper insight into the effects and relative importance (RI) of system and loading parameters in regards to structural response behavior. By multiplying the response sensitivities by the parameter nominal/mean values or SDs, the parameter RI in regards to a given structural response quantity can be quantified in a deterministic or probabilistic sense, respectively. This information is of paramount importance, e.g., in taking design decisions or in defining an efficient experimental program to reduce uncertainties in the modeling parameters of a structure specimen.

FOSM PRA

PRA consists of computing the probabilistic characterization of the response of a specific structure, given as input the probabilistic characterization of material, geometric, and loading parameters. An approximate method of PRA is the FOSM method, which estimates mean values (first-order statistical moments), and variances/covariances (second-order statistical moments) of the response quantities of interest by using a first-order Taylor series expansion of the response quantities in terms of the random/uncertain modeling parameters (Haukaas and Der Kiureghian 2004) about a given point in the parameter space. Thus, FOSM requires the knowledge only of the FSSMs of the random parameters and provides estimates of the FSSMs of the response quantities of interest, also known as response parameters or engineering demand parameters (EDPs). It is noteworthy that often statistical information about the random parameters is limited to FSSMs. In this case, PRA methods that are more advanced than FOSM analysis (e.g., methods based on the full probability distribution) cannot be fully exploited.

In the sequel of this paper, upper case letters $\boldsymbol{\Theta}$, Θ, $\mathbf{R}$, and R will denote random quantities and the corresponding lower case letters $\boldsymbol{\theta}$, θ, $\mathbf{r}$, and r will denote specific realizations. The bold font is used to denote vector and matrix quantities, while the regular font denotes scalar quantities. Given a vector of n random parameters $\boldsymbol{\Theta}$, the corresponding covariance matrix is given by $\mathbf{C}_{\boldsymbol{\Theta}}=[\rho_{ij}\sigma_i\sigma_j]$ $(i,j=1,2,\ldots,n)$, where $\rho_{ij}=$correlation coefficient of random parameters Θ_i and Θ_j with $\rho_{ii}=1$, and $\sigma_i=$SD of random parameter Θ_i. FOSM analysis is based on a linearization of the computed response vector $\mathbf{R}$ of the m response quantities of interest, i.e., $\mathbf{R}$ is approximated by the following first-order truncation of its Taylor series expansion in the random parameters $\boldsymbol{\Theta}$ about a given point $\boldsymbol{\theta}_0$:

$$\mathbf{R}(\boldsymbol{\Theta}) \approx \mathbf{R}_{\mathrm{Lin}}(\boldsymbol{\Theta}) = \mathbf{r}(\boldsymbol{\theta}_0) + \nabla_{\boldsymbol{\theta}}\mathbf{r}|_{\boldsymbol{\theta}=\boldsymbol{\theta}_0}(\boldsymbol{\Theta} - \boldsymbol{\theta}_0) \qquad (1)$$

The mean point, $\boldsymbol{\theta}_0=\boldsymbol{\mu}_{\boldsymbol{\Theta}}$, is an optimal linearization point for estimating the response mean $\boldsymbol{\mu}_{\mathbf{R}}$, independent from the functional relation and joint probability-density function (PDF) of the parameters (Barbato 2007). Using the mean-centered FOSM method, Eq. (1) becomes

$$\mathbf{R}(\mathbf{\Theta}) \approx \mathbf{R}_{\text{Lin}}(\mathbf{\Theta}) = \mathbf{r}(\boldsymbol{\mu}_\mathbf{\Theta}) + \nabla_\boldsymbol{\theta} \mathbf{r}|_{\boldsymbol{\theta}=\boldsymbol{\mu}_\mathbf{\Theta}}(\mathbf{\Theta} - \boldsymbol{\mu}_\mathbf{\Theta}) \qquad (2)$$

The FSSMs of the response quantities $\mathbf{R}$ are approximated by the corresponding moments of the linearized response quantities $\mathbf{R}_{\text{Lin}}$, i.e. (Haukaas and Der Kiureghian 2004; Barbato 2007)

$$\boldsymbol{\mu}_\mathbf{R} \approx \boldsymbol{\mu}_{\mathbf{R}_{\text{Lin}}} = \mathbf{r}(\boldsymbol{\mu}_\mathbf{\Theta}) \qquad (3)$$

$$\mathbf{C}_\mathbf{R} \approx \mathbf{C}_{\mathbf{R}_{\text{Lin}}} = \nabla_\boldsymbol{\theta} \mathbf{r}|_{\boldsymbol{\theta}=\boldsymbol{\mu}_\mathbf{\Theta}} \cdot \mathbf{C}_\mathbf{\Theta} \cdot (\nabla_\boldsymbol{\theta} \mathbf{r}|_{\boldsymbol{\theta}=\boldsymbol{\mu}_\mathbf{\Theta}})^T \qquad (4)$$

The approximate response statistics computed through Eqs. (3) and (4) are extremely important in evaluating the variability of EDPs due to the intrinsic uncertainty of the modeling parameters and provide information on the statistical correlation between different EDPs. These approximate FSSMs can be readily obtained when response sensitivities evaluated at the mean values of the random parameters are available. FOSM-based PRA requires only a single FE analysis, when using DDM-based FE RSA. In the following, only mean-centered FOSM analysis will be considered and referred to as FOSM analysis.

PRA Using MCS

PRA can also be performed via MCS (Liu 2001). In this study, MCS is used to assess the accuracy of the FOSM approximations in Eqs. (3) and (4) when applied to nonlinear FE response analysis of structural and/or soil-structure systems characterized by random/uncertain material parameters and subjected to quasi-static POA. The MCS procedure requires the following three steps. (1) Generation of N realizations of the n-dimensional random parameter vector $\mathbf{\Theta}$ according to a given n-dimensional joint PDF. (2) Computation of N push-over curves (i.e., force-response curves) for each of the m components of the response vector $\mathbf{R}$. These push-over curves are obtained by performing N FE analyses, corresponding to the N realizations of $\mathbf{\Theta}$. Each FE analysis provides m push-over curves, one for each component of $\mathbf{R}$. (3) Statistical estimation through ensemble averaging of specified marginal and joint moments of the components of $\mathbf{R}$ at each load step of the FE response analysis.

MCS is a general and robust methodology for PRA, but it suffers two significant limitations. (1) MCS requires knowledge of the joint PDF of $\mathbf{\Theta}$. In general, this joint PDF is only partially known. Thus, appropriate models, consistent with the incomplete statistical information available (i.e., first- and second-order moments), must be used to generate realizations of the vector $\mathbf{\Theta}$. (2) MCS requires performing N FE response analyses. This number N can be very large for accurate estimates of marginal and joint moments of response quantities $\mathbf{R}$ and increases rapidly with the order of the moments. For real-world structures, complex nonlinear FE analyses are necessary for accurate prediction of structural response and repeating these analyzes a large number of times could be computationally prohibitive.

In this study, the Nataf model (Ditlevsen and Madsen 1996) is used as joint PDF to generate realizations of the random parameters $\mathbf{\Theta}$. It requires specification of the marginal PDFs of random parameters $\mathbf{\Theta}$ and their correlation coefficients and, thus, is able to reproduce the given FSSMs of $\mathbf{\Theta}$.

## Estimation of Response Probability Distributions

The FOSM method used in this paper allows evaluating the uncertainty of the EDPs of interest due to the variability of each random parameter taken separately. This paper presents two simplified procedures, based on FE responses and response sensitivities computed at the parameter mean values, to evaluate the effect of each random material parameter on the uncertainty/randomness of the EDPs considered.

The first procedure (referred to as FOSM-based RI ranking in the sequel) provides the RI ranking of the random material parameters based on FOSM-DDM analysis. Three different RI rankings are obtained: (1) RI ranking based on sensitivities normalized in the deterministic sense, i.e., multiplied by the nominal/mean value of the sensitivity parameter and divided by the mean of the response quantity: $\partial r_j / \partial \theta_i|_{\boldsymbol{\theta}=\boldsymbol{\mu}_\mathbf{\Theta}} \cdot (\mu_{\Theta_i} / \mu_{R_j})$ (referred to as "elasticity" in the optimization literature); (2) RI ranking based on sensitivities normalized in the probabilistic sense, i.e., multiplied by the SD of the sensitivity parameter and divided by the mean of the response quantity: $\partial r_j / \partial \theta_i|_{\boldsymbol{\theta}=\boldsymbol{\mu}_\mathbf{\Theta}} \cdot (\sigma_{\Theta_i} / \mu_{R_j})$; and (3) RI ranking based on the relative marginal contributions of the random material parameters to the total variance of the response, i.e., $(\Delta \sigma_{R_j}^2)_{\Theta_i} / \sigma_{R_j}^2 = [\partial r_j / \partial \theta_i|_{\boldsymbol{\theta}=\boldsymbol{\mu}_\mathbf{\Theta}} \cdot \sigma_{\Theta_i}]^2 / \sigma_{R_j}^2$. The response mean and variance in the three proposed RI rankings are estimated through FOSM analysis. The sensitivities normalized in the deterministic sense represent the percent change in the response due to one percent change in the nominal value of the sensitivity parameter considered. The sensitivities normalized in the probabilistic sense represent the percent change in the mean response due to a change in the mean of the random parameter taken as one percent of the parameter SD, assuming this change to be equally likely for all random parameters.

The so-called "swing" (Porter et al. 2002), referred to hereafter as "swing$_{\text{min-max}}$," is also commonly used to define RI ranking of the uncertain/random parameters in influencing the variability of the response quantities considered. The term swing denotes the variation in an EDP due to the variation of a single parameter with all the other parameters remaining fixed at their corresponding mean/nominal values. Herein, the swing$_{\text{min-max}}$ is computed in correspondence of the minimum and maximum values of the parameter considered when its probability distribution is defined over a finite interval (e.g., β and uniform distributions) or of the 10 and 90% fractiles when its probability distribution is defined over an infinite (e.g., normal distribution) or semiinfinite (e.g., lognormal or exponential distributions) interval. The swing$_{\text{min-max}}$ is estimated based on the FOSM method using the DDM-based response sensitivities multiplied by the appropriate parameter variation (FOSM-DDM analysis). These approximate results are compared with those obtained by repeating the nonlinear FE analysis at the lower and upper bounds of the considered material parameters (swing analysis). The RI ranking of the uncertain/random parameters is also represented graphically via tornado diagrams (Porter et al. 2002). This study also considers the swing corresponding to a parameter variation of ± 1 SD about the mean, referred to as "swing$_{\pm 1 \text{ SD}}$."

The second procedure [referred to as FOSM-based marginal cumulative distribution functions (CDF)/PDF procedure in the sequel] is employed to find an approximation of the CDFs and/or PDFs of the EDPs considered as functions of each uncertain/random parameter considered one at a time. These approximations are obtained assuming that the EDPs have the same distribution as the random parameter considered, with mean and SD estimated through FOSM analysis. This assumption implies
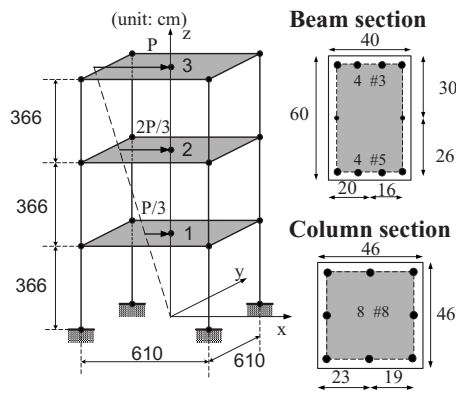
Fig. 1. Geometry, cross-sectional properties, and applied horizontal loads for the three-story RC frame building

Table 1. Marginal PDFs of Material Parameters for the Three-Story RC Frame Building Example

R.V. (unit)	Distribution	Mean	COV (%)
$f_{c,\text{core}}$ (MPa)	Lognormal	34.47	20
$\varepsilon_{c,\text{core}}$ (-)	Lognormal	0.005	20
$f_{\text{cu,core}}$ (MPa)	Lognormal	24.13	20
$\varepsilon_{\text{cu,core}}$ (-)	Lognormal	0.020	20
$f_{c,\text{cover}}$ (MPa)	Lognormal	27.58	20
$\varepsilon_{c,\text{cover}}$ (-)	Lognormal	0.002	20
$\varepsilon_{\text{cu,cover}}$ (-)	Lognormal	0.006	20
f_y (MPa)	β	307.46	10.6
E_0 (MPa)	Lognormal	201,000	3.3
B (-)	Lognormal	0.02	20

that the EDP is considered or approximated as a linear function of the random parameters. These approximate CDFs and/or PDFs are compared with the corresponding probability distributions obtained theoretically from the probability distribution of the random parameter and the nonlinear mapping between the material parameter and the response quantity of interest (principle of conservation of probability). This mapping is obtained by simulating repeatedly the system response (EDPs) for a discrete set of values of the considered material parameter, in the same range used to define the swing, while keeping all the other random parameters fixed at their mean values.

Application Examples

Three-Dimensional RC Frame Building

Deterministic and Probabilistic Structural Model Description

The first application example considered herein consists of a three-dimensional RC frame building on rigid foundation with concrete slabs at each floor as shown in Fig. 1. The frame has three stories of height $h=3.66$ m (12 ft) and one bay of span $L=6.10$ m (20 ft) in each direction. Beam and column cross sections are shown in Fig. 1. Beams and columns are modeled using displacement-based Euler-Bernoulli frame elements with four Gauss-Legendre integration points each. Each column and beam is discretized into two and three frame elements, respectively. Beam and column element cross sections are discretized in fibers of confined concrete, unconfined concrete, and steel reinforcement. The reinforcing steel is modeled through the bilinear hysteretic model, while the concrete is modeled by the Kent-Scott-Park model with zero tension stiffening (Scott et al. 1982). Different material parameters are used for the confined (core) and unconfined (cover) concrete in the columns and beams. The concrete slabs are modeled through a diaphragm constraint at each floor to enforce rigid in-plane behavior.

A total of 11 material constitutive parameters are used to characterize the various structural materials, i.e., four parameters for the confined concrete ($f_{c,\text{core}}$=peak strength; $\varepsilon_{c,\text{core}}$=strain at peak strength; $f_{\text{cu,core}}$=residual strength; and $\varepsilon_{\text{cu,core}}$=strain at which the residual strength is reached), four parameters for the unconfined concrete ($f_{c,\text{cover}}$, $\varepsilon_{c,\text{cover}}$, $f_{\text{cu,cover}}$, $\varepsilon_{\text{cu,cover}}$), and three parameters for the reinforcing steel (E_0=initial stiffness; f_y=yield strength; and b=postyield to initial stiffness ratio). Ten of these material

parameters are modeled as random variables (i.e., spatially fully correlated random fields over the structure), while the residual strength of the unconfined concrete, $f_{\text{cu,cover}}$, is taken as deterministic and equal to zero. Table 1 provides the marginal probability distribution, mean, and coefficient of variation (COV) of each of the random material parameters as obtained from studies reported in the literature (Mirza and MacGregor 1979; Mirza et al. 1979). All material parameters are lognormally distributed with exception of f_y, which follows a β distribution defined by lower limit $f_{y,\text{min}}=227.53$ MPa, upper limit $f_{y,\text{max}}=427.48$ MPa, and shape parameters $\alpha=3.2$ and $\beta=4.28$. Based on engineering judgment, the correlation coefficients of the various pairs of material parameters are assumed as follows: $\rho=0.8$ for (1) $f_{c,\text{core}}$ and $f_{\text{cu,core}}$; (2) $\varepsilon_{c,\text{core}}$ and $\varepsilon_{\text{cu,core}}$; (3) $f_{c,\text{core}}$ and $f_{c,\text{cover}}$; (4) $\varepsilon_{c,\text{cover}}$ and $\varepsilon_{\text{cu,cover}}$; (5) $\varepsilon_{c,\text{core}}$ and $\varepsilon_{c,\text{cover}}$; and (6) $\varepsilon_{\text{cu,core}}$ and $\varepsilon_{\text{cu,cover}}$; $\rho=0.64$ for (1) $f_{\text{cu,core}}$ and $f_{c,\text{cover}}$; (2) $\varepsilon_{c,\text{core}}$ and $\varepsilon_{\text{cu,cover}}$; and (3) $\varepsilon_{c,\text{cover}}$ and $\varepsilon_{\text{cu,core}}$; and $\rho=0$ for all other pairs of parameters. The assumed covariance matrix is a real symmetric positive definite matrix.

Probabilistic POA

After static application of the gravity loads (assumed as uniformly distributed load $q=8$ kN/m^2 at each floor), the structure is subjected to a quasi-static POA, in which an upper triangular distribution of horizontal forces is applied to the master nodes of the floor diaphragm constraints in the x-direction (see Fig. 1). The total base shear force, $P_{\text{tot}}=2P$, is taken as deterministic and increases from 0 to 600 kN during the POA, using a force-control procedure with fixed load increments of 6 kN. Response and DDM-based response sensitivities are evaluated at the mean values μ_Θ of the random parameters Θ. An MCS analysis based on 1,000 realizations is carried out using the Nataf model to generate the joint PDF of Θ. Averaged sensitivities of EDPs **R** are evaluated through central FD analysis, perturbing one material parameter at a time by ±1 SD. Finally, the swing of the EDPs is computed by performing two additional FE analyses for each random material parameter, namely at its upper and lower values as defined previously. FE response, response sensitivity, and probabilistic response computations are performed using the object-oriented FE analysis framework OpenSees (Mazzoni et al. 2007) in which new classes were added to perform MCS-based PRA (Barbato 2007), three-dimensional frame elements were augmented to enable DDM-based RSA (Barbato et al. 2006) and the response sensitivity algorithm for imposing multipoint constraints was implemented (Q. Gu et al., "Consistent tangent moduli for multiyield-surface J_2 plasticity material model," Computational Mechanics, under review, 2010).
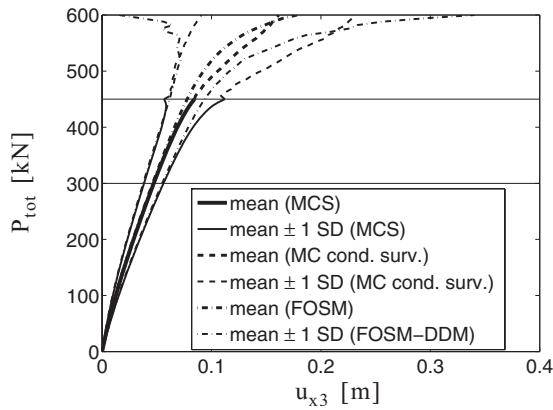
Fig. 2. Probabilistic (first- and second-moment) estimates of the roof displacement in the *x*-direction, u_{x3}, for the three-story RC frame building

Fig. 3. Estimates of the standard deviation of u_{x3} for the three-story RC frame building

Discussion of PRA Results

Fig. 2 shows a comparison of estimates of the mean and mean ±1 SD of the horizontal force-roof displacement in the *x*-direction, u_{x3}, obtained through FOSM-DDM analysis and MCS, respectively. The COV of $\mu_{u_{x3}}$ based on 1,000 simulations is equal to 0.59, 1.04, and 2.85% for P_{tot}=300, 450 and 600 kN, respectively. Thus, the MCS estimates of $\mu_{u_{x3}}$ can be considered an accurate reference solution. For the given structure subjected to quasi-static POA, the failure criterion is defined as nonconvergence of the nonlinear FE analysis or $u_{x3} \geqslant 0.4$ m (i.e., roof drift ratio exceeding 3.65%), whichever happens first. For $P_{tot} \leqslant 450$ kN, no failure case is observed in the MCS performed, while nearly one-third of the Monte Carlo realizations reach failure between load level P_{tot}=450 and 600 kN, respectively. In Fig. 2, the horizontal lines mark the load levels P_{tot}=300 kN (quasi-linear response) and P_{tot}=450 kN (maximum load level without recorded failure cases). The MCS estimates of $\mu_{u_{x3}}$ and $\mu_{u_{x3}} \pm \sigma_{u_{x3}}$ at load levels above P_{tot}=450 kN (denoted in the figures as "MCS cond. surv.") are conditional on the survival of the structural model. The MCS mean response conditional to survival exhibits a stiffening behavior at high load levels (at $P_{tot} > 450$ kN), since it represents the mean response of only the realizations corresponding to structures with high stiffness and/or strength. It is clear that the MCS results conditional to survival cannot be directly compared with the FOSM approximations because of the different meaning of the two sets of FSSM estimates of the response quantity u_{x3}. On the other hand, unconditional MCS results cannot be computed for $P_{tot} > 450$ kN due to nonconverging FE analysis cases. Fig. 2 shows that the FOSM approximation of $\mu_{u_{x3}}$ is in excellent agreement with the MCS results when the structural response is quasi-linear (for $P_{tot} \leqslant 300$ kN), while the FOSM results slightly underestimate the MCS results when the structure undergoes low-to-moderate nonlinear inelastic behavior (for $300 \text{ kN} \leqslant P_{tot} \leqslant 450$ kN).

Fig. 3 displays the estimates of $\sigma_{u_{x3}}$ obtained through: (1) MCS (based on 1,000 realizations); (2) FOSM analysis using DDM-based sensitivities (i.e., FOSM-DDM analysis); and (3) FOSM analysis using the central FDM with perturbations $\Delta\theta_i = \pm \sigma_i$ ($i=1, 2, \ldots, 10$) to compute the response sensitivities. The SD estimates obtained using FOSM analysis combined with the DDM and central FDM, respectively, are very close for $P_{tot} \leqslant 550$ kN. However, the computational cost of the response sensitivities obtained using the DDM is only about 20% that of the two additional nonlinear FE analyses required by the central FDM
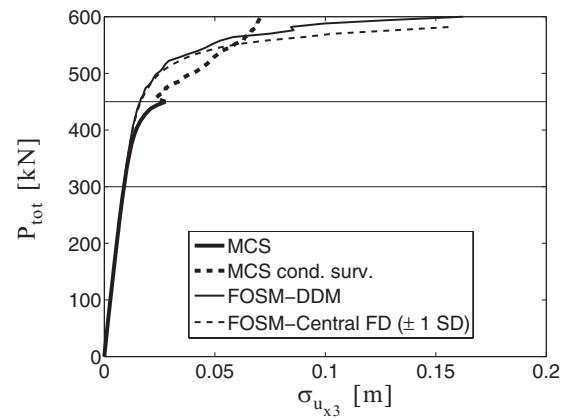
for each sensitivity parameter. In addition, the FE analysis corresponding to parameter $f_{c,core}=\mu_{f_{c,core}}-\sigma_{f_{c,core}}$ does not converge for $P_{tot} > 582$ kN (at load level P_{tot}=582 kN, u_{x3}=0.334 m for $f_{c,core}=\mu_{f_{c,core}}-\sigma_{f_{c,core}}$). Thus, the response SD cannot be estimated from central FD analysis for $P_{tot} \geqslant 582$ kN. Fig. 3 shows that, for this first application example, FOSM-DDM analysis provides, at low computational cost, very good estimates of the SD of EDPs when the structural response exhibits low-to-moderate levels of inelastic behavior. In this specific example, the CPU time required by MCS-based PRA is about 200 times the CPU time required by FOSM-DDM PRA.

RI of Random Material Parameters

Table 2 provides the sensitivities of u_{x3} as EDP to all random material parameters, normalized in the deterministic sense, i.e., $\partial u_{x3}/\partial\theta_i|_{\theta=\mu_\Theta} \cdot \mu_{\Theta_i}/\mu_{u_{x3}}$, and in the probabilistic sense, i.e., $\partial u_{x3}/\partial\theta_i|_{\theta=\mu_\Theta} \cdot \sigma_{\Theta_i}/\mu_{u_{x3}}$, respectively (with the mean response $\mu_{u_{x3}}$ estimated using FOSM). These normalized sensitivities increase in absolute value with increasing load level P_{tot}, except for the normalized sensitivities to $\varepsilon_{c,cover}$, which are first positive and relatively large at P_{tot}=300 kN, decrease in absolute value at P_{tot}=450 kN and become negative at P_{tot}=600 kN. Displacement response sensitivities to parameter $\varepsilon_{c,cover}$ are contributed positively by concrete cover fibers that did not reach their peak strength (since larger values of $\varepsilon_{c,cover}$ lead to smaller stresses for a given strain smaller than $\varepsilon_{c,cover}$) and negatively by concrete cover fibers that entered the post peak response (since larger values of $\varepsilon_{c,cover}$ lead to larger stresses for a given strain larger than $\varepsilon_{c,cover}$). Table 2 also provides the relative marginal contribution, at different load levels, of each random material parameter to the total variance $\sigma^2_{u_{x3}}$ (expressed as percent of $\sigma^2_{u_{x3}}$) estimated using FOSM analysis. In this case, the most important parameter in the probabilistic sense is $f_{c,cover}$ at P_{tot}=300 kN and P_{tot}=450 kN, while $f_{c,core}$ becomes the dominant parameter at P_{tot}=600 kN. The steel material parameters f_y and E are found to affect the structural response u_{x3} relatively less in the probabilistic sense than in the deterministic sense, since their COVs are significantly smaller than the COVs of other parameters. FOSM analysis provides also the contributions to $\sigma^2_{u_{x3}}$ due to the cross terms for all pairs of correlated parameters at different load levels. The interested reader is referred elsewhere (Gu et al. 2010) for the complete presentation of these cross-term contributions to $\sigma^2_{u_{x3}}$. In this application example, the normalized (dimensionless) cross-term contributions to $\sigma^2_{u_{x3}}$ increase for increasing P_{tot} and are of mag-

Table 2. DDM-Based Normalized Sensitivities of u_{x3} to Material Parameters and Parameter Relative Contribution to Variance of u_{x3} at Different Load Levels (Three-Story RC Frame Building Example)

P_{tot} (kN)	$(\partial u_{x3}/\partial\theta_i)\|_{\vartheta=\mu_\Theta}\cdot(\mu_{\Theta_i}/\mu_{u_{x3}})$			$(\partial u_{x3}/\partial\theta_i)\|_{\vartheta=\mu_\Theta}\cdot(\sigma_{\Theta_i}/\mu_{u_{x3}})$			$\Delta(\sigma^2_{u_{x3}})/\sigma^2_{u_{x3}}$ (%)		
	300	450	600	300	450	600	300	450	600
$f_{c,core}$	−0.230	−0.313	−2.742	−0.046	−0.063	−0.548	6.01	9.22	36.21
$\varepsilon_{c,core}$	0.219	0.284	1.540	0.044	0.057	0.308	5.42	7.44	11.42
$f_{cu,core}$	0	0	−0.006	0	0	−0.001	0	0	<0.01
$\varepsilon_{cu,core}$	0	0	−0.003	0	0	−0.001	0	0	<0.01
$f_{c,cover}$	−0.521	−0.605	−1.737	−0.104	−0.121	−0.347	30.74	33.74	14.53
$\varepsilon_{c,cover}$	0.413	0.305	−0.160	0.083	0.061	−0.032	19.30	8.56	0.12
$\varepsilon_{cu,cover}$	0	−0.006	−1.142	0	−0.001	−0.228	0	<0.01	6.28
f_y	0	−0.063	−2.070	0	−0.007	−0.219	0	0.10	5.80
E	−0.369	−0.417	−0.765	−0.012	−0.014	−0.025	0.42	0.44	0.08
b	0	0	−0.047	0	0	−0.010	0	0	0.01

nitude comparable to or even larger than the marginal contributions of the random parameters to the response variance. In particular, the statistical correlation of parameters $f_{c,core}$ and $f_{c,cover}$ ($\rho=0.8$) yields the highest contribution to $\sigma^2_{u_{x3}}$ at $P_{tot}=600$ kN (i.e., 36.70%). This phenomenon has a physical intuitive explanation. The value of $f_{c,cover}$ determines the force level at which spalling of the cover concrete initiates, i.e., the lower $f_{c,cover}$, the sooner spalling initiates. Also, the sooner and the more extensively spalling initiates, the more stress is redistributed to the core concrete. Finally, the lower $f_{c,core}$, the more likely is crushing of the core concrete in compression and consequently the higher is the deformation of the structure. Similar considerations can be made for the case of jointly high values of $f_{c,cover}$ and $f_{c,core}$, leading to lower deformations of the structure. The high positive correlation of $f_{c,cover}$ with $f_{c,core}$ (two parameters representing the same physical property of concrete, but differing only because of the lack or presence of confinement) produces the high cross-term contribution to $\sigma^2_{u_{x3}}$ of the two parameters, due to the chain effect described above. Furthermore, at $P_{tot}=600$ kN, the sum of the marginal and cross-term contributions of $f_{c,cover}$

and $f_{c,core}$ accounts for 87.44% of $\sigma^2_{u_{x3}}$. It is concluded that the concrete strength is the most influential factor on the deformation of this benchmark structure at high load levels.

Fig. 4 compares the RI of the random material parameters in regards to u_{x3} at different load levels (i.e., $P_{tot}=300$, 450, and 600 kN) through tornado diagrams. The RI is expressed as the relative change in the response u_{x3} corresponding to the parameters' lower and upper bounds (swing$_{min-max}$). The relative change in the response for each parameter is computed by FOSM-DDM analysis and by swing analysis.

From Figs. 4(a and b), it is observed that the FOSM-DDM estimate of the swing$_{min-max}$ of the response parameter u_{x3} is accurate for low-to-moderate level of inelastic behavior in the structural response. In this range of inelastic behavior, the considered EDP is only moderately sensitive to parameter variations, with max(Δu_{x3})/$u_{x3}=14.5\%$ at $P_{tot}=300$ kN and max(Δu_{x3})/$u_{x3}=18.3\%$ at $P_{tot}=450$ kN. For high level of inelastic behavior [$P_{tot}=600$ kN, see Fig. 4(c)], discrepancies occur between swing results obtained using FOSM-DDM and swing analyzes, in particular for $f_{c,core}$, $f_{c,cover}$, $\varepsilon_{c,core}$, $\varepsilon_{cu,cover}$, and f_y. For these param-
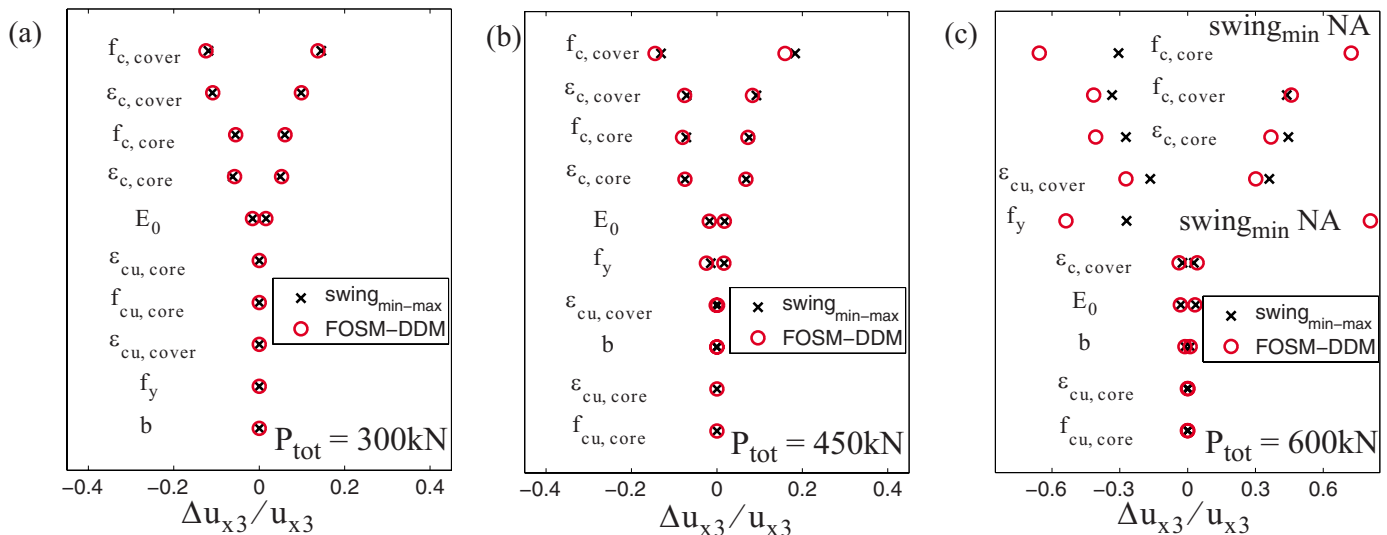

Fig. 4. Tornado diagrams of the variability (swing$_{min-max}$) of u_{x3} due to parameter variability for the three-story RC frame building: (a) $P_{tot}=300$ kN; (b) $P_{tot}=450$ kN; and (c) $P_{tot}=600$ kN
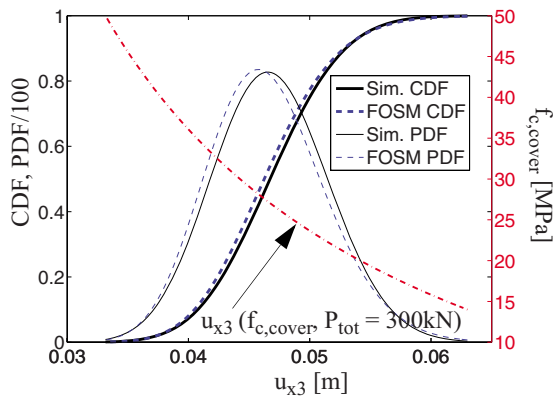
Fig. 5. CDF and PDF of u_{x3} due to randomness of $f_{c,\text{cover}}$ only and mapping between $f_{c,\text{cover}}$ and u_{x3} for the three-story RC frame building ($P_{\text{tot}}=300$ kN)

Fig. 6. CDF and PDF of u_{x3} due to randomness of $f_{c,\text{cover}}$ only and mapping between $f_{c,\text{cover}}$ and u_{x3} for the three-story RC frame building ($P_{\text{tot}}=450$ kN)

eters, the FOSM-DDM estimates of the EDP variations are very large (72.4% for $f_{c,\text{core}}$, 45.8% for $f_{c,\text{cover}}$, 40.6% for $\varepsilon_{c,\text{core}}$, 30.1% for $\varepsilon_{cu,\text{cover}}$, and 80.8% for f_y). These FOSM-DDM estimates of the EDP variations underestimate the exact EDP variations at the parameters' upper bounds and overestimate the exact EDP variations at the parameters' lower bounds. Thus, the FOSM-DDM estimates of swing$_{\text{min-max}}$ capture only partially the asymmetric change in the response (with respect to the response computed at the mean values of the parameters) due to the nonlinear relation between response and material parameters. For the parameters f_y and $f_{c,\text{core}}$, to which the response is most sensitive at load level $P_{\text{tot}}=600$ kN, the FE analyses at the parameters' lower bounds do not converge due to singularity of the structure stiffness matrix at $P_{\text{tot}}=576$ kN and $P_{\text{tot}}=588$ kN, respectively. These results are denoted in Fig. 4(c) as "swing$_{\text{min}}$ NA" (NA=not available) and suggest a highly nonlinear relation between the response u_{x3} and material parameters f_y and $f_{c,\text{core}}$. In order to generate the tornado diagrams in Fig. 4 using swing analysis, two additional nonlinear FE POAs are required for each random parameter. On the other hand, the tornado diagrams based on FOSM-DDM analysis results are obtained as a by-product of the original nonlinear FE POA performed in conjunction with FE RSA at the mean values of the random parameters. Tornado diagrams based on swing analysis do not provide any information about the effects of statistical correlation between random parameters. In contrast, FOSM analysis also provides information about response variance dependency on parameter statistical correlation (Gu et al. 2010). The tornado diagrams in Fig. 4 based on FOSM-DDM analysis are consistent with those based on swing analysis in terms of RI ranking of the material parameters, with the only exception of FOSM-DDM analysis underestimating the RI of f_y at $P_{\text{tot}}=600$ kN. Similar results, not presented here due to space constraints, were obtained for the RI ranking based on swing ± 1 SD (Gu et al. 2010).

Compared to the information provided by a tornado diagram, FOSM analysis provides additional information about correlation between different EDPs and between EDPs and material parameters. Due to space limitations, such correlation results are not shown here and the interested reader is referred elsewhere (Barbato 2007). It was found that FOSM-based and MCS-based PRA results are in excellent agreement for low-to-moderate level of inelastic behavior, including the statistical correlation between different response quantities (EDPs) and between response quantities and material parameters.
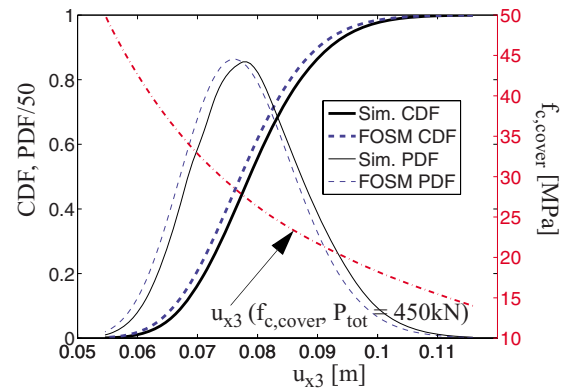
Approximate PDFs/CDFs of Response Parameters due to Randomness of Single Material Parameter

Figs. 5–7 compare the PDF (scaled down by a factor 100, 50, and 10) and CDF of u_{x3} for $P_{\text{tot}}=300$, 450, and 600 kN, respectively, obtained by the proposed simplified FOSM-based estimation procedure with their counterparts (denoted by "Sim. PDF/CDF" in Figs. 5–7) obtained theoretically from the probability distribution of $f_{c,\text{cover}}$ and the nonlinear mapping between $f_{c,\text{cover}}$ and u_{x3}. This mapping was obtained by repeating the nonlinear FE POA for 20 different values of $f_{c,\text{cover}}$ (uniformly spaced over the interval 14–50 MPa) while keeping all the other parameters fixed and by subsequently interpolating the values of u_{x3} obtained through simulation with a cubic spline. The obtained mapping between $f_{c,\text{cover}}$ and u_{x3} is also plotted in Figs. 5–7. The proposed simplified procedure provides an approximation of the PDF/CDF of the EDP u_{x3} due to the randomness of $f_{c,\text{cover}}$ (as only source of uncertainty) at a negligible computational cost after an FOSM-DDM analysis is performed at the mean values of the random material parameters. This simplified procedure is exact for a one-to-one linear mapping between the considered model parameter and EDP. In this specific example for $P_{\text{tot}}=300$ kN and $P_{\text{tot}}=450$ kN, the mapping between $f_{c,\text{cover}}$ and u_{x3} is one-to-one, smooth, and not far from linear, especially in the range of $f_{c,\text{cover}}$ over the body of the PDF of $f_{c,\text{cover}}$, which leads to a good approximation for the FOSM-DDM based PDF/CDF of u_{x3}. From the results presented
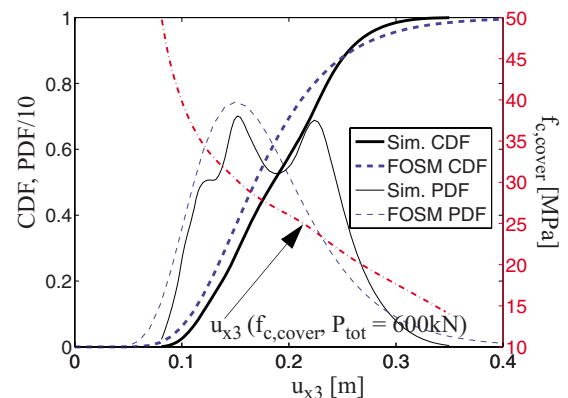
Fig. 7. CDF and PDF of u_{x3} due to randomness of $f_{c,\text{cover}}$ only and mapping between $f_{c,\text{cover}}$ and u_{x3} for the three-story RC frame building ($P_{\text{tot}}=600$ kN)
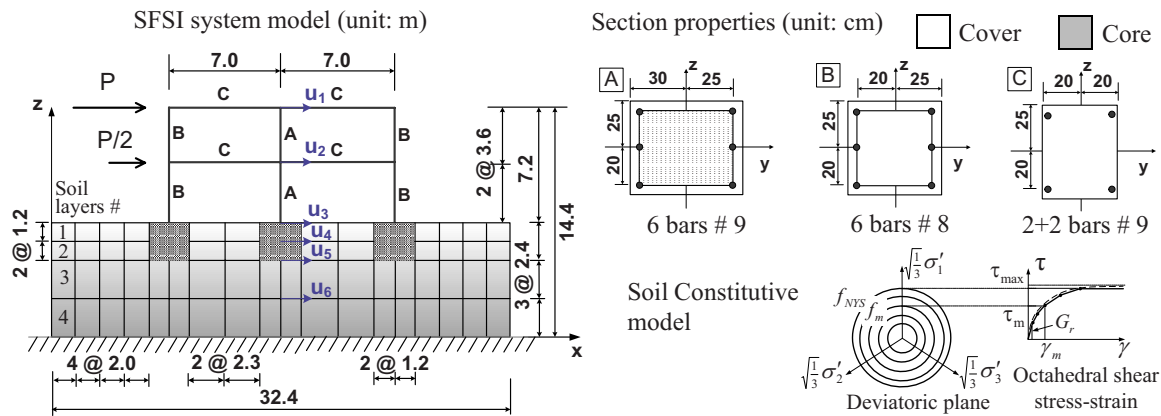
Fig. 8. Two-dimensional model of the SFSI system: geometry, section properties, soil FE mesh, and soil constitutive model

in Figs. 5 and 6 and from results corresponding to the other random material parameters not presented here due to space limitations (Barbato 2007), it is found that the proposed simplified procedure provides at very low computational cost a reasonably good approximation for the PDF/CDF of EDPs (due to the randomness of a single parameter as only source of uncertainty) at low-to-moderate levels of inelastic behavior. At high level of inelastic behavior (e.g., at $P_{tot}=600$ kN), the approximate PDFs/CDFs can be significantly inaccurate, as shown in Fig. 7. In this specific example at $P_{tot}=600$ kN, the PDF of u_{x3} obtained through the nonlinear mapping between $f_{c,cover}$ and u_{x3} is bimodal and, thus, very different from the approximate lognormal distribution assumed by the proposed approximate method. In general, the inaccuracy of the FOSM-DDM based PDF/CDF for high levels of inelastic behavior is due to the following reasons: (1) FOSM based estimates of response mean and SD are inaccurate and (2) the mapping between FE model parameter and EDP is highly nonlinear and sometimes not even one-to-one.

Two-Dimensional SFSI System

Deterministic and Probabilistic SFSI System Model Description

The second application example consists of a two-dimensional model of a soil-foundation-structure interaction (SFSI) system shown in Fig. 8. The structure is a two-story two-bay RC frame with section properties given in Fig. 8. The foundation consists

of isolated RC footings below each column. The soil is a layered clay with stiffness and strength properties varying with depth. The frame structure of this SFSI system is modeled using displacement-based Euler-Bernoulli frame FEs with distributed plasticity, each with four Gauss-Legendre integration points. Section stress resultants at the monitored cross sections are computed by using a two-dimensional fiber (i.e., layer) section discretization. Foundation footings and soil layers are modeled through isoparametric four-node quadrilateral plane strain FEs with bilinear displacement interpolation. The soil mesh is shown in Fig. 8. The soil domain is assumed under plane strain conditions with a constant soil thickness of 4.0 m, equal to the interframe distance. The constitutive behavior of the reinforcement steel is modeled through the one-dimensional J_2 plasticity model with kinematic and isotropic linear hardening (Conte et al. 2003). The concrete is modeled using the Kent-Scott-Park model with zero tension stiffening (Scott et al. 1982). The soil is modeled using a pressure-independent multiyield-surface J_2 plasticity material model (Gu et al. 2009b; Q. Gu et al., "Consistent tangent moduli for multiyield-surface J_2 plasticity material model," *Computational Mechanics*, under review, 2010), specialized for plane strain condition (Fig. 8). Different material parameters are used for the confined (core) and unconfined (cover) concrete in the columns and beams, and for the four soil layers.

Twelve material parameters are used to characterize the various structural materials employed in the frame model, i.e., four parameters for the confined concrete ($f_{c,core}$, $\varepsilon_{c,core}$,

Table 3. Mean and COV of Structural and Soil Material Parameters (with Assumed Lognormal Distributions) for the Two-Dimensional SFSI System

Structural material parameters			Soil material parameters		
R.V. (unit)	Mean	COV (%)	R.V. (unit)	Mean	COV (%)
$f_{c,core}$ (MPa)	34.49	20	τ_1 (kPa)	33	25
$\varepsilon_{c,core}$ (-)	0.004	20	G_1 (kPa)	54,450	30
$f_{cu,core}$ (MPa)	20.69	20	τ_2 (kPa)	26	25
$\varepsilon_{cu,core}$ (-)	0.014	20	G_2 (kPa)	33,800	30
$f_{c,cover}$ (MPa)	27.59	20	τ_3 (kPa)	35	25
$\varepsilon_{c,cover}$ (-)	0.002	20	G_3 (kPa)	61,250	30
$\varepsilon_{cu,cover}$ (-)	0.008	20	τ_4 (kPa)	44	25
f_y (MPa)	248.20	10.6	G_4 (kPa)	96,800	30
E_0 (MPa)	200,000	3.3	—	—	—
H_{kin} (MPa)	1,612.9	20	—	—	—

Table 4. Parameter Relative Marginal Contribution (%) to Variance of u_1 ($\sigma_{u_1}^2$) at Different Load Levels (Two-Dimensional SFSI System)

	Structural material parameters				Soil material parameters		
P_{tot} (kN)	450	547.5	750	P_{tot} (kN)	450	547.5	750
$f_{c,\text{core}}$	1.09	1.07	1.18	τ_1	<0.01	<0.01	<0.01
$\varepsilon_{c,\text{core}}$	0.95	0.8	0.70	G_1	0.02	0.02	<0.01
$f_{cu,\text{core}}$	0	0	0	τ_2	<0.01	<0.01	<0.01
$\varepsilon_{cu,\text{core}}$	0	0	0	G_2	0.02	0.02	<0.01
$f_{c,\text{cover}}$	44.31	46.15	34.44	τ_3	<0.01	<0.01	<0.01
$\varepsilon_{c,\text{cover}}$	29.83	25.94	4.22	G_3	0.05	0.03	<0.01
$\varepsilon_{cu,\text{cover}}$	0	0	0.03	τ_4	<0.01	<0.01	<0.01
f_y	0.86	4.10	46.91	G_4	<0.01	<0.01	<0.01
E_0	3.18	2.81	0.25	—	—	—	—
H_{kin}	<0.01	<0.01	0.01	—	—	—	—

$f_{cu,\text{core}}$, $\varepsilon_{cu,\text{core}}$), the unconfined concrete ($f_{c,\text{cover}}$, $\varepsilon_{c,\text{cover}}$, $\varepsilon_{cu,\text{cover}}$, with $f_{cu,\text{cover}}=0$ MPa assumed as deterministic), and the reinforcing steel [f_y, E_0, H_{kin} (kinematic hardening modulus), and $H_{\text{iso}}=0$ MPa (isotropic hardening modulus assumed as deterministic)]. Ten of these material parameters are assumed to follow lognormal distributions with mean and COV given in Table 4. The statistical correlation coefficients between various structural material parameters are the same as in the first application example. In addition to the 12 structural material parameters, eight material parameters are used to characterize the four soil layers, i.e., the shear strength, τ_i, and initial (low strain) shear modulus, G_i, with $i=1,2,3,4$, corresponding to the numbering of the soil layers (from top to bottom, see Fig. 8). These eight soil material parameters are also assumed to follow lognormal distributions with mean and COV given in Table 3 (Phoon and Kulhawy 1996). Based on engineering judgment, the statistical correlation coefficients of the various pairs of soil material parameters are assumed as follows: $\rho=0.4$ for (1) $\tau_1-\tau_2$; (2) τ_1-G_1; (3) $\tau_2-\tau_3$; (4) τ_2-G_2; (5) $\tau_3-\tau_4$; (6) τ_3-G_3; and (7) τ_4-G_4; and $\rho=0$ for all other parameter pairs.
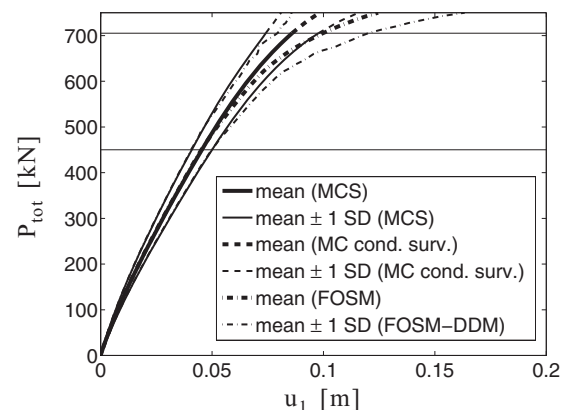
Probabilistic POA

After static application of the gravity loads for both the structure and the soil, the structure is subjected to a quasi-static POA, with an upper triangular distribution of horizontal forces applied at the floor levels (Fig. 8). The total base shear force, $P_{\text{tot}}=1.5P$, is taken as deterministic and increases from 0 to 750 kN during the POA, using a force-control procedure with fixed load increments of 7.5 kN. System response and DDM-based response sensitivities are computed at the mean values $\boldsymbol{\mu_\Theta}$ of the random parameters $\boldsymbol{\Theta}$. An MCS analysis based on 1,000 simulations is performed using the Nataf model as joint PDF of the random parameters $\boldsymbol{\Theta}$ (with COV of μ_{u_1} equal to 0.20, 0.49, and 0.91% for $P_{\text{tot}}=450$, 547.5, and 750 kN, respectively). Averaged sensitivities of the response quantities **R** are evaluated through central FD analysis, perturbing one material parameter at a time by ± 1 SD. FE response, response sensitivity, and probabilistic response computations are performed using OpenSees (Mazzoni et al. 2007), in which the constitutive model for the soil was augmented for DDM-based RSA (Gu et al. 2009b).

Discussion of PRA Results

Fig. 9 shows a comparison of estimates of the mean and mean ± 1 SD of the horizontal force-roof displacement (u_1) response (with u_1 evaluated at the top of the central column, see Fig. 8), obtained

through FOSM-DDM analysis and MCS, respectively. Fig. 10 displays the estimates of σ_{u_1} obtained through: (1) MCS based on 1,000 realizations; (2) FOSM-DDM analysis; and (3) FOSM analysis using the central FDM with perturbations $\Delta\theta_i=\pm\sigma_i$ ($i=1,\ldots,20$) to compute the response sensitivities. For the given structure subjected to quasi-static POA, the condition of failure is defined as nonconvergence of the FE computation due to singularity of the structure stiffness matrix or $u_1 \geq 0.28$ m (i.e., roof drift ratio exceeding 4.0%), whichever happens first. For $P_{\text{tot}} \leq 547.5$ kN, no failure case is observed in the MCS performed, while nearly one-quarter of the Monte Carlo realizations reach failure between load levels $P_{\text{tot}}=547.5$ and 750 kN, respectively. In Figs. 9 and 10, the horizontal lines mark the load levels $P_{\text{tot}}=450$ kN (quasi-linear response) and $P_{\text{tot}}=547.5$ kN (largest applied load for which no simulation realization fails). For $P_{\text{tot}} > 547.5$ kN, the MCS estimates of μ_{u_1} and σ_{u_1} conditional on the survival of the structure (MCS cond. surv.) are plotted. The results obtained using FOSM and MCS are qualitatively similar to those presented for the first application example. Fig. 9 shows that the FOSM approximation of μ_{u_1} is in excellent agreement with the MCS results when the system response is quasi-linear (for $P_{\text{tot}} \leq 450$ kN). The FOSM results slightly underestimate the MCS results when the system undergoes low-to-moderate inelastic deformations (for $450 \text{ kN} \leq P_{\text{tot}} \leq 547.5$ kN), with discrepancy between FOSM and MCS results increasing for increasing level of inelastic behavior. In this second example, the maximum level

Fig. 9. Probabilistic (first- and second-moment) estimates of the roof displacement, u_1, for the two-dimensional SFSI system
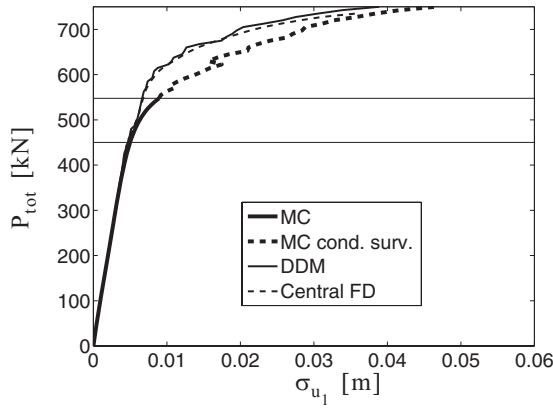
**Fig. 10.** Estimates of the standard deviation of u_1 for the two-dimensional SFSI system

---

of inelastic structural deformation reached in the analysis is lower than in the first application example. Therefore, the discrepancies between FOSM and MCS analysis results are also smaller than in the first example. Fig. 10 shows that FOSM-central FD based analysis overestimates the MCS estimate of σ_{u_1}, while the FOSM-DDM based estimate of σ_{u_1} nearly coincides with the MCS estimate for $P_{tot} \leqslant 500$ kN. As in the first application example, FOSM analysis provides, at very low computational cost, very good estimates of the mean and SD of EDPs for low-to-moderate levels of inelastic response of the system.

RI of Random Material Parameters

Table 4 provides the relative marginal contributions to $\sigma_{u_1}^2$ of each of the material random parameters, expressed as percentage of $\sigma_{u_1}^2$, at different load levels. The percent contributions to $\sigma_{u_1}^2$ due to the cross terms for all pairs of correlated structural material parameters at different load levels have also been computed and presented elsewhere (Gu et al. 2010). The cross terms for soil material parameters are negligible, with contributions to $\sigma_{u_1}^2$ smaller than 0.01%. From the results presented in Table 4, the following observations are made. (1) The parameter $f_{c,cover}$ has the largest marginal contribution to $\sigma_{u_1}^2$ at load levels $P_{tot}=450$ kN

and $P_{tot}=547.5$ kN and has the second largest contribution at $P_{tot}=750$ kN. The relative marginal contribution of $\varepsilon_{c,cover}$ to $\sigma_{u_1}^2$ is very important at lower load levels and decreases dramatically with increasing load. The observations made for the first application example regarding the displacement response sensitivity to parameter $\varepsilon_{c,cover}$ also apply here. Thus, the structural response strongly depends on the cover concrete material parameters, in particular at low-to-moderate levels of inelastic deformations. (2) The concrete parameters $f_{cu,core}$ and $\varepsilon_{cu,core}$ do not influence the response, since at the mean values of all random parameters, the core concrete does not reach its peak strength in any fiber into which the structure is discretized during the POA. (3) The relative marginal contribution of f_y to $\sigma_{u_1}^2$ increases drastically with the load level. It is almost negligible at load level $P_{tot}=450$ kN at which very few steel reinforcement fibers have yielded, while it becomes the largest contribution to $\sigma_{u_1}^2$ at load level $P_{tot}=750$ kN. In particular, at $P_{tot}=750$ kN, the marginal relative contribution of f_y to $\sigma_{u_1}^2$ is $(\Delta\sigma_{u_1}^2)_{f_y}/\sigma_{u_1}^2=46.9\%$. (4) The variability of the soil properties has an almost negligible effect on the variability of the response parameter u_1 and this effect decreases for increasing load levels. It is noteworthy that in this example SFSI effects manifest themselves very differently under static and dynamic loading conditions. In particular, for the same SFSI system as the one used here, the structural response is much more sensitive to changes in the soil material parameters under dynamic load conditions (earthquake base excitation) than under static load conditions (Gu et al. 2009a). In addition, the effects on $\sigma_{u_1}^2$ of the statistical correlation between the random parameters are small and decrease with increasing load level. Only the statistical correlations between $\varepsilon_{c,core}$ and $\varepsilon_{c,cover}$ and between $f_{c,core}$ and $f_{c,cover}$ have nonnegligible effects on $\sigma_{u_1}^2$ (Gu et al. 2010).

Fig. 11 shows the tornado diagrams of swing$_{min-max}$ for the EDP u_1 at different load levels ($P_{tot}=450$, 547.5, and 750 kN) for the 10 parameters affecting u_1 the most. The complete tornado diagrams can be found elsewhere (Gu et al. 2010). These tornado diagrams provide the material parameter RI ranking expressed as relative change in the response due to perturbation of each model parameter while all other parameters are kept at their mean values. This relative response change is computed by FOSM-
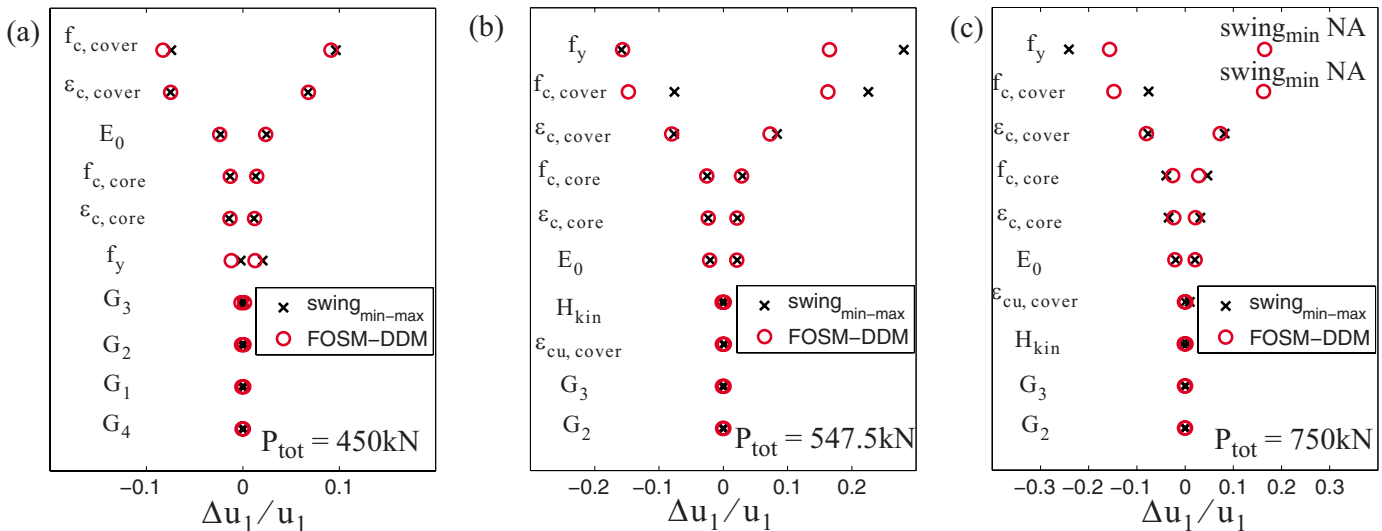
Fig. 11. Tornado diagrams of the variability of u_1 (swing$_{min-max}$) due to parameter variability for the two-dimensional SFSI system: (a) P_{tot} =450 kN; (b) P_{tot}=547.5 kN; and (c) P_{tot}=750 kN
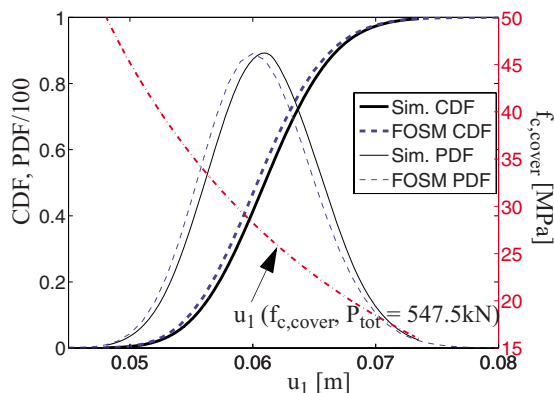
Fig. 12. CDF and PDF of u_1 due to randomness of $f_{c,\text{cover}}$ only and mapping between $f_{c,\text{cover}}$ and u_1 for the two-dimensional SFSI system: $P_{\text{tot}}=547.5$ kN

DDM analysis and by swing analysis. The effects of parameter variability on response variability increase for increasing load level. The tornado diagrams based on FOSM-DDM analysis are close to those based on swing analysis (repeated FE analysis) at $P_{\text{tot}}=450$, 547.5, and 750 kN, except for the two most important parameters (f_y and $f_{c,\text{cover}}$) at $P_{\text{tot}}=750$ kN. In spite of these discrepancies, the parameter RI ranking obtained from FOSM-DDM analysis matches that obtained from swing analysis.

Approximate PDFs/CDFs of Response Parameters due to Randomness of Single Material Parameter

Fig. 12 compares the PDFs and CDFs of u_1 due to the randomness of $f_{c,\text{cover}}$ as only source of uncertainty for $P_{\text{tot}}=547.5$ kN. Results relative to other load levels can be found elsewhere (Gu et al. 2010). These PDFs/CDFs are obtained: (1) from the proposed simplified FOSM-DDM based procedure and (2) theoretically from the probability distribution of the parameter $f_{c,\text{cover}}$ and the nonlinear mapping between $f_{c,\text{cover}}$ and u_1 (obtained through FE simulation). Fig. 12 also plots the cubic spline interpolated mapping between $f_{c,\text{cover}}$ and u_1. As in the previous example, the proposed simplified procedure provides at very low computational cost a reasonably good approximation for the PDF/CDF of the EDP u_1 (due to the randomness of a single parameter as only source of uncertainty) at low-to-moderate levels of inelastic behavior ($P \leqslant 547.5$ kN). At high level of inelastic behavior (e.g., $P_{\text{tot}}=750$ kN), the approximate PDF/CDF become significantly inaccurate for the same reasons mentioned in the previous example.

Conclusions

This paper compares two different PRA methods based on nonlinear FE response and RSA, namely the mean-centered FOSM approximation and MCS. These two PRA methods are used to compute the FSSMs of the response of: (1) a three-dimensional RC frame building model and (2) a two-dimensional SFSI system model, both subjected to quasi-static POA. Use of different methods for computing the FE response sensitivities employed in FOSM analysis, namely the DDM and the central FD method, are also investigated in this study. From the results presented, it is found that the FOSM method with response sensitivities computed using the DDM (FOSM-DDM analysis) provides, at very low computational cost, very good estimates of the mean and SD

of response quantities for low-to-moderate levels of nonlinear inelastic behavior in the response of structural and SFSI systems subjected to quasi-static POA. The RI ranking in both the deterministic and probabilistic sense of the material parameters on the structural or SFSI system response is obtained as by-product of a FOSM-DDM analysis at negligible additional computational cost. The FOSM results are used directly to obtain approximate PDFs/CDFs of response quantities due to the randomness of a single material parameter as only source of uncertainty (i.e., with all other random parameters kept constant at their mean values). In the examples considered, these approximate probability distributions are in fair to good agreement (in the low-to-moderate range of nonlinear inelastic behavior of the structure or system) with the exact distributions obtained theoretically from the probability distribution of the random material parameter considered and the computationally expensive FE simulated mapping between this material parameter and the response quantity of interest. For high level of inelastic behavior in the structure or system considered, the agreement between FOSM and MCS results (for mean and SD of response parameter) deteriorates and the two proposed approximate methods (i.e., FOSM-DDM based RI ranking and the FOSM-DDM based marginal CDF/PDF procedure) can be used to obtain only qualitative information, such as RI ranking of the material parameters in influencing the response variability. It is noteworthy that unconditional MCS estimates of response mean and SD are not available when nonlinear FE analyses corresponding to specific realizations of the parameter vector do not converge due to singularity of the structure stiffness matrix or other numerical difficulties. From the results presented in this paper, it is observed that FOSM-DDM analysis provides at very low computational cost a satisfactorily accurate simplified PRA method for structural and SFSI systems subjected to quasi-static POA, provided that the level of inelastic behavior of the structure or SFSI system is limited to low-to-moderate. At high level of inelastic deformations, FOSM-DDM can still be used effectively to obtain qualitative information on the RI ranking of modeling parameters on the system response.

Acknowledgments

References

Applied Technology Council (ATC). (1996). "Seismic evaluation and retrofit of concrete buildings." *Rep. No. ATC-40*, Redwood City, CA.

Applied Technology Council (ATC). (2005). "Improvement of nonlinear static seismic analysis procedures." *Rep. No. ATC-55*, Redwood City, CA.

Barbato, M. (2007). "Finite-element response sensitivity, probabilistic response and reliability analyses of structural systems with applications to earthquake engineering." Ph.D. dissertation, Dept. of Structural Engineering, Univ. of California at San Diego, La Jolla, CA.

Barbato, M., and Conte, J.P. (2005). "Finite-element response sensitivity analysis: A comparison between force-based and displacement-based frame element models." *Appl. Mech. Eng.*, 194(12–16), 1479–1512.

Barbato, M., and Conte, J. P. (2006). "Finite-element structural response sensitivity and reliability analyses using smooth versus non-smooth material constitutive models." *Int. J. Reliab. Saf.*, 1(1–2), 3–39.

Barbato, M., Gu, Q., and Conte, J. P. (2006). "Response sensitivity and probabilistic response analyses of reinforced concrete frame structures." *Proc., 8th National Conf. on Earthquake Engineering* (CD-ROM).

Barbato, M., Zona, A., and Conte, J. P. (2007). "Finite-element response sensitivity analysis using three-field mixed formulation: General theory and application to frame structures." *Int. J. Numer. Methods Eng.*, 69(1), 114–161.

Bjerager, P. (1990). "On computation methods for structural reliability analysis." *Struct. Safety*, 9(2), 79–96.

Bolotin, V. V. (1968). *Statistical methods in structural mechanics*, Holden-Day, Inc., San Francisco.

Chinese Building Press (CBP). (2001). "Code for seismic design of buildings." *GB 50011-2001*, Beijing (in Chinese).

Conte, J. P., Barbato, M., and Spacone, E. (2004). "Finite-element response sensitivity analysis using force-based frame models." *Int. J. Numer. Methods Eng.*, 59(13), 1781–1820.

Conte, J. P., Jagannath, M. K., and Meghella, M. (1995). "Earthquake response sensitivity analysis of concrete gravity dams." *Proc., 7th Int. Conf. on Applications of Statistics and Probability*, 395–402.

Conte, J. P., Vijalapura, P. K., and Meghella, M. (2003). "Consistent finite-element response sensitivity analysis." *J. Eng. Mech.*, 129(12), 1380–1393.

Crandall, S. H. (2006). "A half-century of stochastic equivalent linearization." *Struct. Control Health Monit.*, 13(1), 27–40.

Der Kiureghian, A., and Ke, B.-J. (1988). "The stochastic finite-element method in structural reliability." *Probab. Eng. Mech.*, 3(2), 83–91.

Ditlevsen, O., and Madsen, H. O. (1996). *Structural reliability methods*, Wiley, New York.

Dong, W. M., Chiang, W. L., and Wong, F. S. (1987). "Propagation of uncertainties in deterministic systems." *Comput. Struct.*, 26(3), 415–423.

European Committee for Standardization (ECS). (2005). "Eurocode 8—Design of structures for earthquake resistance." *EN1998*, Brussels, Belgium.

BSCC. (1997). "NEHRP recommended provisions for seismic regulations for new buildings and other structures." *FEMA 302-303*, Washington, D.C.

Ghanem, R. G., and Spanos, P. D. (1991). *Stochastic finite elements: A spectral approach*, Springer, New York.

Grigoriu, M. (2000). "Stochastic mechanics." *Int. J. Solids Struct.*, 37(1–2), 197–214.

Gu, Q., Barbato, M., and Conte, J. P. (2009a). "Handling of constraints in finite-element response sensitivity analysis." *J. Eng. Mech.*, 135(12), 1427–1438.

Gu, Q., Barbato, M., and Conte, J. P. (2010). "Probabilistic push-over response analysis of structural and/or geotechnical systems." *Rep. No. SSRP-2010/01*, Dept. of Structural Engineering, Univ. of California, San Diego, San Diego.

Gu, Q., Conte, J. P., Elgamal, A., and Yang, Z. (2009b). "Finite-element response sensitivity analysis of multi-yield-surface J_2 plasticity model by direct differentiation method." *Comput. Methods Appl. Mech. Eng.*, 198(30–32), 2272–2285.

Haftka, R. T., and Gurdal, Z. (1993). *Elements of structural optimization*, Kluwer, Dordrecht, Germany.

Haukaas, T. (2006). "Efficient computation of response sensitivities for inelastic structures." *J. Struct. Eng.*, 132(2), 260–266.

Haukaas, T., and Der Kiureghian, A. (2004). "Finite-element reliability and sensitivity methods for performance-based engineering." *Rep. No. PEER 2003/14*, Pacific Earthquake Engineering Research Center, Univ. of California, Berkeley, Berkeley, CA.

Haukaas, T., and Der Kiureghian, A. (2005). "Parameter sensitivity and importance measures in nonlinear finite-element reliability analysis." *J. Eng. Mech.*, 131(10), 1013–1026.

Kleiber, M., Antunez, H., Hien, T. D., and Kowalczyk, P. (1997). *Parameter sensitivity in nonlinear mechanics: Theory and finite-element computation*, Wiley, New York.

Liu, J. S. (2001). *Monte Carlo strategies in scientific computing. Springer series in statistics*, Springer, Berlin.

Lupoi, G., Franchin, P., Lupoi, A., and Pinto, P. E. (2006). "Seismic fragility analysis of structural systems." *J. Eng. Mech.*, 132(4), 385–395.

Mazzoni, S., McKenna, F., and Fenves, G. L. (2007). *OpenSees command language manual*, Pacific Earthquake Engineering Research Center, Univ. of California at Berkeley, CA, ⟨http://opensees.berkeley.edu/OpenSees/manuals/usermanual/OpenSeesCommandLanguageManual.pdf⟩ (August 2010).

Mirza, S. A., and MacGregor, J. G. (1979). "Variability of mechanical properties of reinforcing bars." *J. Struct. Div.*, 105(5), 921–937.

Mirza, S. A., MacGregor, J. G., and Hatzinikolas, M. (1979). "Statistical descriptions of strength of concrete." *J. Struct. Div.*, 105(6), 1021–1037.

Phoon, K. K., and Kulhawy, F. H. (1996). "On quantifying inherent soil variability." *Proc., ASCE GED Spec. Conf. on Uncertainty in the Geologic Environment: From Theory to Practice*, Vol. 1, ASCE, Reston, VA, 326–340.

Porter, K. A., Beck, J. L., and Shaikhutdinov, R. V. (2002). "Sensitivity of building loss estimates to major uncertain variables." *Earthquake Spectra*, 18(4), 719–743.

Saltelli, A., Chan, K., and Scott, E. M. (2000). *Sensitivity analysis*, Wiley, Chichester, U.K.

Scott, B. D., Park, P., and Priestley, M. J. N. (1982). "Stress-strain behavior of concrete confined by overlapping hoops at low and high-strain rates." *J. Am. Concr. Inst.*, 79(1), 13–27.

To, C. W. S. (2001). "On computational stochastic structural dynamics applying finite elements." *Arch. Comput. Methods Eng.*, 8(1), 3–40.

Zona, A., Barbato, M., and Conte, J. P. (2005). "Finite-element response sensitivity analysis of steel-concrete composite beams with deformable shear connection." *J. Eng. Mech.*, 131(11), 1126–1139.

Zona, A., Barbato, M., and Conte, J. P. (2006). "Finite-element response sensitivity analysis of continuous steel-concrete composite girders." *Steel Compos. Struct.*, 6(3), 183–202.